The following publication F. Zhang et al., "Battery ESS Planning for Wind Smoothing via Variable-Interval Reference Modulation and Self-Adaptive SOC Control Strategy," in IEEE Transactions on Sustainable Energy, vol. 8, no. 2, pp. 695-707, April 2017 is available at https://doi.org/10.1109/TSTE.2016.2615638.

Battery ESS Planning for Wind Smoothing via Variable-interval Reference Modulation and Self-adaptive SOC Control Strategy

Feng Zhang, *Member, IEEE*, Ke Meng, *Member, IEEE*, Zhao Xu, *Senior Member, IEEE*, Zhaoyang Dong, *Senior Member, IEEE*, Li Zhang, Can Wan, *Member, IEEE*, and Jun Liang

Abstract—**The variability of wind power generation increases the uncertainties in modern power system, affecting its physical operation. Owning to fast response capability, battery energy storage system (BESS) has offered an answer to this problem. In this paper, a novel sizing methodology is proposed for BESS planning, which strikes a balance between economic cost and wind smoothing performance. Firstly, a novel variable-interval reference signal optimization approach and a fuzzy control-based charging/discharging scheme are presented to smooth wind power, maintaining the state-of-health of BESS in the meanwhile. And then, power and energy capacities are determined according to a statistical model of charge/discharge power and the economic cost model respectively. Finally, case studies are carried out to demonstrate the performance of the proposed method. The impact from wind power forecasting error during real-time operation is also analyzed.**

Index Terms—**Energy storage, wind power, capacity, SOC, optimization.**

NOMENCLATURE

Reference Power Calculation

P_t^w	Annual historical wind power (MW).
P_i^{ref}	Reference output of the i^{th} interval (MW).
$(t_{i-1},t_i]$	The i^{th} time interval.
M	Variance of the actual and reference wind power.
Δt_{cyc}	Trading period of real-time electricity market.
t_{max}	Maximum time inteval duration.
P^c_{max}	Maximum charge power indicated as positive (MW).
P^d_{max}	Maximum discharge power indicated as negative (MW).
σ^d	Discharge powre loss.
σ^c	Charge power loss.

Self-adaptive SOC Control of BESS

SOC_t	Instantaneous SOC value.
P_t^c	Charge power for fluctuation smoothing (MW).
P_t^d	Discharge power for fluctuation smoothing (MW).
γ_t	Power adjustment coefficient.
SOC_{ref}	Ideal SOC value.
ΔSOC	Offset between SOC_t and SOC_{ref} .

Methodology for BESS Capacity Planning

F	Probability function.
P^c_{rat}, P^d_{rat}	Rated charge and discharge power (MW).
C_{fun}	Fundamental cost ($ / MWh).
χ	Construction cost per unit size ($ / MWh).
ψ	Maintenance cost per unit size ($ / MWh).
int	Annual interest rate.
g	Annual inflation rate.
N	Lifetime of BESS in years.
V_{rat}	Rated energy capacity of BESS (MWh).
C^p_{SOC}, C^p_{Pow}	Penalty costs when SOC or power limits are violated.
C_{adj}	Cost caused by the power adjustment.
pr_i	Electricity price of the i^{th} interval
α, β	Per unit cost of the over-charged/-discharged energy.
n	Total number of the times when $SOC_t > S_h^3$.
$[p_i^c, q_i^c]$	i^{th} time interval when $SOC_t > S_h^3$.
m	Total number of the times when $SOC_t < S_{min}$.
$[p_j^d, q_j^d]$	j^{th} time interval when $SOC_t < S_{min}$.
η, φ	Unit cost of energy when BESS charges/discharges over rated power ($ / MWh) .
z	Total number of times when the charge power is larger than P^c_{rat}.
$[e_i^c, f_i^c]$	i^{th} time interval when the charge power is larger than P^c_{rat} .
s	Total number of times when the discharge power is larger than P^d_{rat}.
$[e_j^d, f_j^d]$	j^{th} time interval when the discharge power is larger than P^d_{rat}.
Δt	Time duration of each sampling interval.
ΔT_i	Time duration of i^{th} interval of reference output
δ	Per unit cost of curtailed wind energy ($ / MWh).

This work was supported in part by the National Natural Science Foundation of China under Grant 51307101, 71401017, and 71420107027, in part by funding from the Faculty of Engineering & Information Technologies, The University of Sydney, under the Faculty Research Cluster Program, and in part by China Southern Power Grid Funding under Grant WYKJ00000027.

F. Zhang, L. Zhang and J. Liang are with the Key Laboratory of Power System Intelligent Dispatch and Control, Ministry of Education, Shandong University, Jinan, 250061, China (e-mail: fengzhang@sdu.edu.cn).

K. Meng and Z.Y. Dong are with the School of Electrical and Information Engineering, The University of Sydney, NSW 2006, Australia (e-mail: kemeng@ieee.org, zydong@ieee.org).

Z. Xu is with the Department of Electrical Engineering, The Hong Kong Polytechnic University, Hong Kong, China (e-mail: eezhaoxu@polyu.edu.hk).

C. Wan is with the College of Electrical Engineering, Zhejiang University, Hangzhou, 310027, China (email: can.wan@ieee.org).

v	Total number of power adjustments resulting in wind power curtailment.
$[x_i^c, y_i^c]$	i^{th} time interval when wind power is curtailed by power adjustment.
ε	Per unit cost of the shortage of discharge power ($/MWh).
w	Total number of adjustments resulting in shortage of discharge power.
$[x_j^d, y_j^d]$	j^{th} time interval when shortage of discharge power is caused by power adjustment.
ΔP_t	Power deviation between the smoothed wind power and reference output (MW).
$\Delta P_{\max}$	Maximum permitted power deviation.
θ	Probability value to guarantee the effectiveness of fluctuation smoothing.
B	Annual wind farm benefit

Improve PSO Calculation

p^i	Best position that the particle *i* has ever visited.
p^g	Best position that the particle subsets have ever visited.
w	An inertia weight.
c_1, c_2	Acceleration coefficients.
γ_1, γ_2	Parameters distributed in the interval [0, 1] at random.
$\Delta\varphi^2$	Variance of solution quality.
c	A constant close to zero.

Case study

P_t^{sw}	Smoothed wind power (MW).
P_t^{ref}	Optimal reference output (MW).
P_t^{cw}	Curtailed wind power (MW).
$[t_0 , t_T]$	Time boundaries of the annual wind power.
nc	Total number of charge intervals in one year
nd	Total number of discharge intervals in one year
$[nc_{oi}, nc_i]$	Time range of i^{th} charge interval
$[nd_{oj}, nd_j]$	Time range of j^{th} discharge interval

I. Introduction

RENEWABLE energy is one of the most promising energy resources for solving global energy crisis [1]. However, these weather-dependent resources exhibit greater uncertainty and variability compared to conventional generation [2]. Many utilities are experiencing challenges in matching consumer demand for electricity and intermittent renewable power generation. Whilst wind power is one of the promising renewable energy sources, it is still treated as a non-dispatchable resource in practice [3]. Owning to the outstanding performance and falling upfront cost, battery energy storage system (BESS) is believed to be most potential for constraining wind power output fluctuation [4]. With BESS, wind power generation can be dispatched as other conventional energy resources to some extent [5]. However, currently large-scale application of BESS is still an applicable but expensive option for power smoothing. Therefore, economic analysis of BESS becomes the focus of this research area [6]. Generally, lowering the BESS capacity requirement and using proper control strategy will significantly improve BESS performance [7],[8]. Consequently, in this paper, a self-adaptive control strategy is proposed for reducing capacity requirement in planning stage.

Capacity determination including energy capacity and power capacity can be categorized into BESS planning. Minimizing BESS capacity can be achieved by considering a specific objective over BESS life cycle with historical data [9]. In [10], a BESS-based operational dispatch scheme for a wind farm was proposed to mitigate the impacts of wind power forecasting error and determine the optimal BESS capacity. A stochastic framework for wind power integration using energy storage systems was proposed in [11]. In [12], sizing and control methodologies were presented to smooth the variability of wind power, and an artificial neural network was adopted in the control strategy to reduce the BESS investment. In general, these studies optimize BESS capacity under certain objective functions, in which wind power is smoothed on an hourly basis. In [13],[14], the reference power output with longer intervals are proposed. The reference power refers to the net output from the combined wind-BESS system, which is a key factor in sizing BESS capacity since the power deviation determines the BESS reference signal [15]. Thus, to lower the capacity requirement, the choice of reference power requires further study. Obviously, hourly-averaged reference signal cannot be tracked effectively. Variable-intervals are more flexible for offset-free tracking. In this paper, the feasibility of variable-interval reference power determination will be analyzed and a novel calculation method will be presented.

Proper charging/discharging control strategy is also a basis for BESS capacity planning. For the best return on investment, it is necessary to extend the life of the size-limited BESS [16]. State-of-charge (SOC) is a measure of energy left in the battery with respect to its nominal capacity. In previous research on the impacts of SOC on BESS life span, depth of discharge (DOD) was introduced to show the drained energy from BESS in one cycle [17]. The curve of cycle life versus DOD was presented in [18], indicating that more nominal cycles can be performed if a cell is discharged with a lower DOD. The BESS control strategy in [9] took DOD, charge/discharge current, rate and cycles into consideration to prolong the lifespan of BESS. To mitigate the risk of energy trading, optimal sizing and allocation methods for BESS were proposed through a cost-benefit analysis model in [19]. In terms of control strategies, specific upper and lower limits were set to keep SOC within proper range to avoid over-charge/-discharge in [20],[21]. In these studies, similarly restrictions on SOC or DOD are taken as measures for BESS protection. However, when SOC approaches limits, a sudden output change may significantly influence the smoothing performance.

For this reason, a novel reference power calculation method and a self-adaptive SOC control strategy are proposed in this paper. The overall framework of the proposed methodology is shown in Fig. 1. It should be noted that on basis of the two essential procedures, i.e., the calculation of reference power and design of control strategy, the power capacity and energy capacity of BESS can be determined accordingly. The rest of this paper is organized as follows. The reference output calculation is introduced in Section II; the self-adaptive SOC control strategy is proposed in Section III; the BESS capacity planning is described in Section IV; the real-time implement of BESS is discussed in Section V; case studies are given in Section VI; and, finally, the conclusion is drawn in SectionVII.

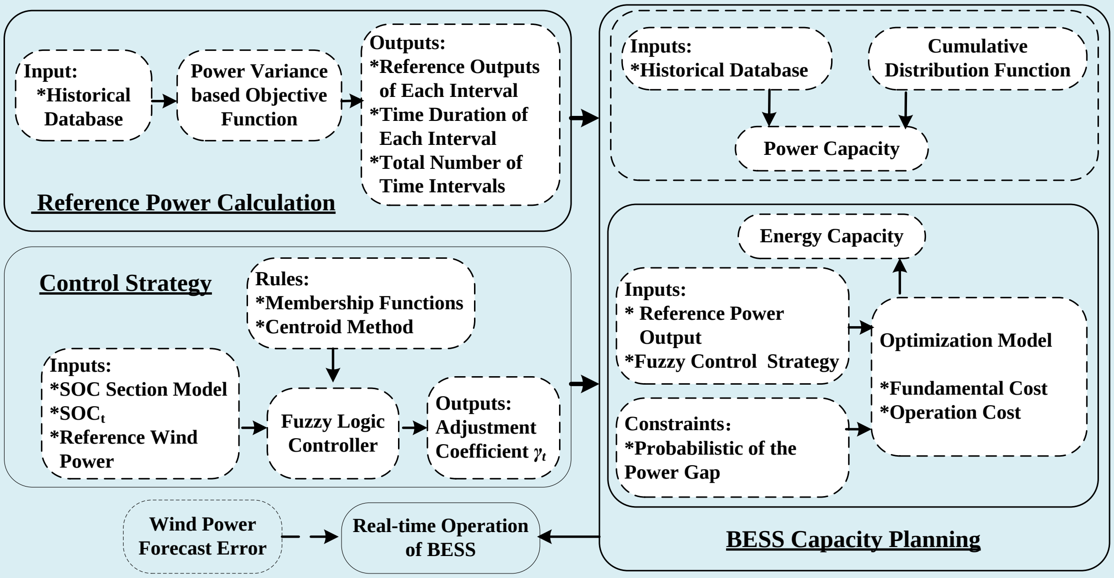

Fig.1. Framework of the capacity planning methodology

II. Optimal Reference Output For Wind Power

The power deviation between the reference and actual wind power output determines the charge/discharge power for BESS, which means the reference signal needs to be calculated first. In previous studies, the reference outputs were formulated as a staircase function with fixed time interval, i.e., one hour, and the reference is an averaged value for that period. However, the replacement of thermal power with renewable generation results in a higher frequency deviation for a given imbalance between supply and demand [22]. In fact, it is more flexible if the time intervals are not fixed, resulting in lower BESS capacity requirement.

Generally the mismatch power between the generation and load of day-ahead market will be addressed in the real-time market. Moreover, with the increase of wind power penetration in the power grid, the thermal power generation in the real-time market will not satisfy the mismatch power. As such, it is a trend for wind power to participate in the real-time market. In this paper, the time interval duration of reference output can be X (X=1, 2, 3…) times of the trading period in real-time electricity market. In this paper, it is assumed that electricity market is dispatched on a fifteen-minute basis [23]. Subsequently, the presented reference output aims to track the variation of wind power by minimizing the deviation between reference and actual output to reduce BESS capacity requirement. The historical wind power data is divided into k intervals, among which the i^{th} interval is represented as P_i^{ref} (i=1, 2…k), and the corresponding time bounds are defined as (t_{i-1}, t_i] (i=1, 2…k). Notably, if k varies, P_i^{ref}, t_{i-1}, and t_i change accordingly. For this reason, an objective function is proposed to determine P_i^{ref} via minimizing the variance of power deviation.

$$\min M = \sum_{i=1}^{k} \frac{\sum_{t=t_{i-1}}^{t_i} \left| P_t^w - P_i^{ref} \right|^2}{t_i - t_{i-1}} \tag{1}$$

This function is subjected to the following constraints:

1) Time limits: The duration of each time interval needs to meet the following requirements

$$t_i - t_{i-1} = X \cdot \Delta t_{cyc} \tag{2}$$

$$\Delta t_{cyc} \le t_i - t_{i-1} \le t_{max} \tag{3}$$

Under various electricity market schemes, the choice of Δt_{cyc} may be different. However, it will not affect the presented reference power calculation method. In this research, Δt_{cyc} , t_{max} are set as fifteen minutes and two hours respectively [23].

2) Power limits: Considering the charge/discharge ability of BESS, the power deviation betweeen reference and actual wind output are constrained as,

$$P_{\max}^d \cdot (1-\sigma^d) \le P_t^w - P_i^{ref} \le \frac{P_{\max}^c}{1-\sigma^c} \tag{4}$$

III. Self-adaptive SOC Control Strategy

After the calculation of reference power, the SOC control strategy for BESS can be designed. Whilst the BESS operation mode can be determined by wind power deviation, an advanced control strategy is required to prolong the life span of BESS. For this purpose, a self-adaptive SOC control strategy based on fuzzy control theory is proposed to avoid potential damages due to over-charge/-discharge.

A. SOC Section Model

In order to constrain the over-charge/-discharge, SOC section model is designed. As shown in Fig. 2, S_{min} and S_{max} are the lower and upper limits, and $S_h^{1,2,3}$ and $S_l^{1,2}$ denote the upper and lower warning limits. When SOC_t exceeds the warning limits, the charge/discharge power will be adjusted to protect BESS.

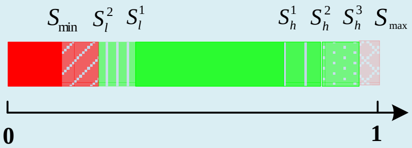

Fig. 2 SOC sections diagram

$$P_t^c = \gamma_t \cdot \left(P_t^w - P_i^{ref}\right) \cdot \left(1 - \sigma^c\right) \tag{5}$$

$$P_t^d = \gamma_t \cdot \frac{P_t^w - P_i^{ref}}{1 - \sigma^d} \tag{6}$$

where, γ_t varies when SOC_t is in different sections, and $0 \leq \gamma_t \leq 1$. It needs to be noted that the determination of γ_t is focus of the self-adaptive control strategy.

B. Determination of γ_t based on Fuzzy Control Theory

The fuzzy logic controller (FLC) is designed to determine γ_t, as shown in Fig. 3.

1) Input: The input variables include SOC_t, SOC_{ref}, P_t^w and P_i^{ref}. $\Delta SOC \in [-0.5, 0.5]$ indicates the over-charge/-discharge. P_t^w and P_i^{ref} determine whether BESS needs to charge or discharge.

2) Fuzzification: Seven fuzzy sets of ΔSOC, i.e., (*PP*, *PN*, *PM*, *ZO*, *NM*, *NN*, and *NP*) are designed. As another group of input variables, P_t^w and P_i^{ref} are used to indicate the charging (NF) and discharging (PF) states. The output γ_t of FLC has five fuzzy sets, i.e., (*RM*, *RC*, *RB*, *RA*, and *RN*). And a triangular membership function is presented in this study to calculate the membership values $\mu_{\Delta SOC}$ and $\mu_{\gamma t}$. Fig. 4 shows the membership functions of the input and output variables. In Fig. 4(a), when SOC_t is lower than 0.15, it is considered to be extremely low and the membership value is set as 1.0 to stop discharging. In Fig. 4(b), γ_t can be decreased to zero in the fuzzy set RM to effectively constrain over-charge/-discharge. When SOC_t is in the normal area, RN is a constant as 1.0 implying no adjustment is needed.

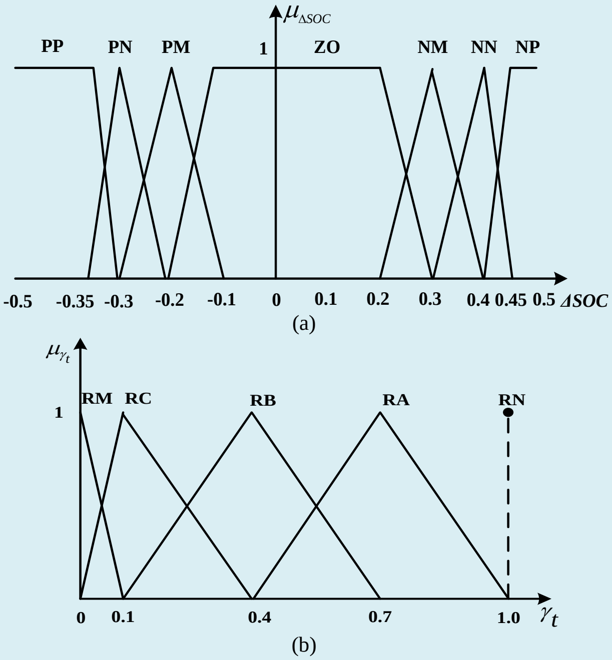

Fig. 4. Membership functions. (a) ΔSOC; (b) γ_t

3) Fuzzy inference: According to the membership functions, fourteen fuzzy control rules, as shown in Table I, are designed on basis of the following principles.

TABLE I
FUZZY RULE MATRIX

	ΔSOC						
	PP	*PN*	*PM*	*ZO*	*NM*	*NN*	*NP*
NF	*RN*	*RN*	*RN*	*RN*	*RA*	*RB*	*RC*
PF	*RM*	*RC*	*RB*	*RN*	*RN*	*RN*	*RN*

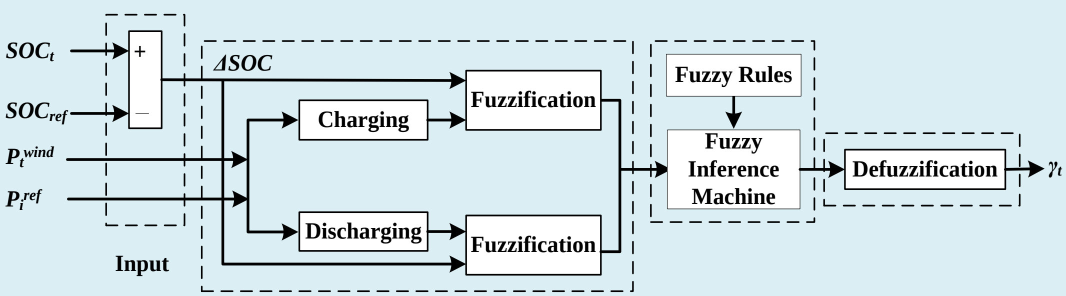

Fig.3. Fuzzy logic controller

If ΔSOC is positive and BESS is charging, then the larger ΔSOC is, the smaller γ_t is to avoid overcharge.

If ΔSOC is in the normal range, regardless of whether BESS is charging or discharging, BESS should provide the required power, implying that γ_t will not be adjusted.

If ΔSOC is negative and BESS is discharging, then the larger ΔSOC is, the smaller γ_t is adjusted.

4) Defuzzification: Based on the comparison of simulation results with other defuzzification strategies, such as the bisector method and maximum method, centroid method is selected in this study as the defuzzification strategy.

IV. BESS Capacity Configuration

After the two essential procedures have been presented, the rated power and energy capacity of BESS can be determined according to the operating conditions of BESS.

A. Power Capacity

The rated power capacity of BESS will be computed with probability density function (pdf) and cumulative distribution function (cdf) of the charge/discharge power [24]. The rated power capacity is expected to meet the charge power and discharge power requirements with the cdf of p ($0< p \leq 1$).

When $0 \leq P_t^w - P_i^{ref} \leq P_{max}^c$,

$$F\left[0 \leq \left(P_t^w - P_i^{ref}\right)\cdot\left(1-\sigma^c\right) \leq P_{rat}^c\right] = p \tag{7}$$

When $P_{max}^d \leq P_t^w - P_i^{ref} \leq 0$,

$$F\left[P_{rat}^d \leq \frac{P_t^w - P_i^{ref}}{1-\sigma^d} \leq 0\right] = p \tag{8}$$

B. Energy Capacity

Considering the high cost of BESS, the rated energy capacity needs to achieve the trade-off between the investment cost and smoothing performance [25]. BESS is mainly used to smooth out wind fluctuations and limit wind power ramping rate as required by power grid. For the owner of wind farm, the goal of installing a BESS is to smooth wind power and thereby maximize its profit. In this research, the energy capacity is planned according to a cost-oriented model with the goal of maximizing the annual wind farm benefit.

1) Annual income: The wind farm income In is mainly obtained by power trading in electricity market

$$In = \sum_{i=1}^{k} P_i^{ref} \cdot \Delta T_i \cdot pr_i \tag{9}$$

2) Cost: The cost of BESS mainly includes the fundamental cost and the operation cost.

a) Fundamental Cost: The fundamental cost is mainly contributed by the construction and maintenance of BESS.

$$C_{fun} = \left(\chi + \psi\right)\cdot V_{rat} \cdot \frac{\left(1+g\right)^N}{\left(1+\mathrm{int}\right)^N} \cdot \frac{1}{N} \tag{10}$$

Here C_{fun} takes the time value of capital into consideration [10]. In terms of BESS lifetime, the equivalent full cycle method is used for estimating the BESS lifetime to failure [10], [19]. The equivalent full cycles are defined as the number of cycles to failure multiplied by the DOD. Afterwards, the average equivalent full cycles is the value for lifetime calculation.

b) Operation Cost: The cost generated during the operation of BESS is introduced to evaluate the operating conditions. When SOC_t exceeds the limits or the charge/discharge power exceeds the rated capacity, potential damages may be incurred to BESS. Therefore, the penalty costs C_{SOC}^p and C_{Pow}^p are considered when SOC or power limits are violated. Moreover, as a result of the adjustment of γ_t, a small amount of wind power has to be curtailed. Meanwhile, the adjustment of discharge power incurs shortage of power to smooth the expected power gap. For this reason, the cost C_{adj} caused by the power adjustment is taken into consideration. Specifically, the operation cost mainly includes C_{SOC}^p, C_{Pow}^p and C_{adj}, which are calculated in the following manner. For simplicity, C_{SOC}^p only considers the severe over-charge/-discharge scenarios, i.e., $SOC_t \geq S_h^3$ and $0 \leq SOC_t \leq S_{min}$.

$$C_{SOC}^p = \alpha \cdot \sum_{i=1}^{n}\sum_{t=p_i}^{q_i}(SOC_t - S_h^3)\cdot V_{rat} + \beta \cdot \sum_{j=1}^{m}\sum_{t=p_j}^{q_j}(SOC_t - S_{\min})\cdot V_{rat} \tag{11}$$

C_{Pow}^p is computed according to the following equation,

$$\begin{aligned} C_{pow}^p = \eta \cdot \sum_{i=1}^{z}\sum_{t=e_i}^{f_i}\left[\gamma_t \cdot \left(P_t^w - P_i^{ref}\right)\cdot\left(1-\sigma^c\right) - P_{rat}^c\right]\cdot \Delta t + \\ \varphi \cdot \sum_{j=1}^{s}\sum_{t=e_j}^{f_j}\left[P_{rat}^d - \gamma_t \cdot \frac{P_t^w - P_i^{ref}}{1-\sigma^d}\right]\cdot \Delta t \end{aligned} \tag{12}$$

C_{adj} is calculated according to the following equation,

$$\begin{aligned} C_{adj} = \delta \cdot \sum_{i=1}^{v}\sum_{t=x_i}^{y_i}\left(1-\gamma_t\right)\cdot\left(P_t^w - P_i^{ref}\right)\cdot \Delta t + \\ \varepsilon \cdot \sum_{j=1}^{w}\sum_{t=x_j}^{y_j}\left(1-\gamma_t\right)\cdot\left|P_t^w - P_i^{ref}\right|\cdot \Delta t \end{aligned} \tag{13}$$

3) Annual benefit: Based on the proposed cost models, the objective function for BESS energy capacity optimization can be formulated as,

$$Max.\ B = \sum_{i=1}^{k} P_i^{ref} \cdot \Delta T_i \cdot pr_i - \left(C_{fun} + C_{SOC}^p + C_{pow}^p + C_{adj}\right) \tag{14}$$

Since C_{fun} and $C_{SOC}^p + C_{pow}^p + C_{adj}$ are mutually constrained, there is a tradeoff between the fundamental cost and the operation cost. Due to the limited size of BESS, the smoothed wind power cannot be identical with the reference output. To guarantee the performance of wind power smoothing, a probabilistic constraint is needed for the objective function,

$$F\left(|\Delta P_t| \leq \Delta P_{max}\right) \geq \theta \tag{15}$$

C. Solution Method

In this study, PSO is selected as solver to compute the rated energy capacity. However, considering the limited searching precision of the original PSO in various complex problems [26], an improved PSO algorithm including the advantages of the shuffled frog leaping algorithm (SFLA) [27] is presented in this paper to increase the search precision and the ability of avoiding local optimal solutions. The detailed modifications are as follows:

1) The form of a subset is introduced as the unit of particle updates to promote the diversity of particle populations and avoid rapid aggregations of particles. All particles are divided into m subsets, each of which contains n particles with a D-dimensional solution space. This algorithm updates the particles' velocities and positions at time step t as follows.

$$V_{t+1}^i = w \cdot V_t^i + c_1 \cdot \gamma_1 \cdot (p^i - X_t^i) + c_2 \cdot \gamma_2 \cdot (p^g - X_t^i) \tag{16}$$

$$X_{t+1}^i = X_t^i + V_{t+1}^i \tag{17}$$

When $V_{t+1}^i \geq V_{max}$, then $V_{t+1}^i = V_{max}$, and when $V_{t+1}^i \leq V_{min}$, then $V_{t+1}^i = V_{min}$. V_{max} and V_{min} are the maximum and minimum velocities which prevent velocity from growing extremely large or small.

2) After generation of the new solutions, particle subsets are released and rebuilt for the next cycle, aiming to increase the competition and avoiding local optimal solutions. Then PSO algorithm updates the velocities and positions iteratively until a stopping criterion is met.

$$\lim_{t\to\infty} \Delta\varphi^2 = c \tag{18}$$

3) In the procedure of subset rebuilding, the solutions of a certain ratio, e.g., 10%, which are of the worst fitness are re-

placed by the solutions with the best fitness to inherit their good features and achieve fast convergence.

On basis of the proposed methodology for BESS capacity planning, the steps for implementation are shown in Fig. 5. It can be noted that the improve PSO can be applied in (1) and (14) for reference output calculation and energy capacity optimization, respectively.

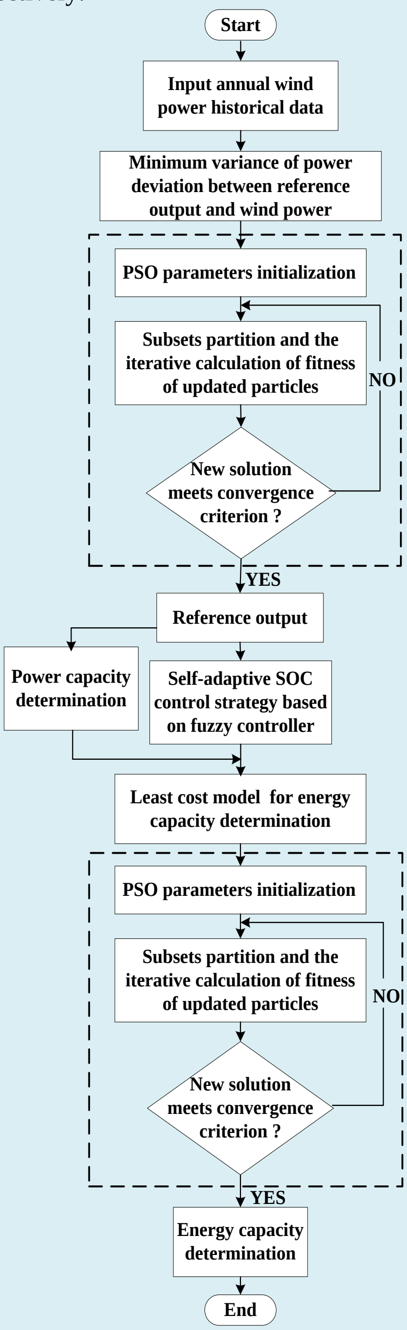

Fig.5. Flowchart of implementation of this method

V. Discussion on Real-time operation of BESS

In order to fully demonstrate the performance of the planned BESS, the real-time operation of BESS is also discussed in this research. In the real-time electricity market, the near-future forecast wind power is needed for market trading.

Besides, in the prevailing markets, once the wind power generation schedule is submitted to the transmission system operator (TSO), the schedule adjustment will not be allowed within predefined hours (say 2 hours) [28]. Consequently the wind power of very short term forecast is necessary for the real-time operation of BESS. Besides, there are also some issues needs to be further considered.

1) Reference output calculation within predefined hours : With the forecast power, the reference output for the predefined hours (say 2 hours) is determined. According to (1)-(4), k, P_i^{ref}, $t_{i\text{-}1}$, and t_i can be calculated for the next 2 hours. In real-time operation, the reference output is the wind power schedule submitted to the TSO from the wind farm. Besides, nowadays wind farms are normally equipped with wind power forecast system, and the rolling forecast of wind power can be carried out and recorded progressively in wind farms. Consequently the forecast data can be achieved by the forecast system in wind farm.

2) Real time control of BESS: In terms of the real time control of BESS, it is the same as the procedure of BESS capacity planning, which means self-adaptive SOC control strategy is still adopted for real-time control of BESS.

3) Wind power forecast error: In fact, there are many choices that are suitable for addressing the forecast error, such as some kind of storage system and other generation units, e.g., diesel generator. Currently the very short term forecast can reach a high precision with an rms error of 10% [29], so the amplitudes of forecast power error will not so high. Besides, it is worth noticing that no matter what measure is taken, forecast power error will be addressed independently from the BESS. Hence there is no coordination of the charging-discharging control between the BESS and other energy storage or generator.

VI. Case Study

The proposed methodology is verified with historical data collected from a 90 MW wind farm located on the southeast coast of Shandong Province in China. The lead-acid battery is selected owning to its excellent economical and technical performance. The typical BESS operation parameters are shown in Table II [24],[30], and parameters of improved PSO algorithm can be referred to [26],[27].

TABLE II
PARAMETER SETTING IN CASE STUDY

BESS operation parameters		
σ^c	Charging loss	0.1
σ^d	Discharging loss	0.05
P^c_{max} (MW)	Maximum charge power	15
P^d_{max} (MW)	Maximum discharge power	-15
p	Value of cpf	0.95
θ	Probabilistic constraint	0.95
ΔP_{max} (MW)	Maximum offset between the smoothed and reference wind power	5
SOC_{ref}	Ideal SOC value	0.5
Int (%)	Annual interest rate	2
g (%)	Annual inflation rate	3
Improved PSO algorithm		
w	Inertia weight	1.1
c_1, c_2	Acceleration coefficients	2.05
c	Convergence criterion	0.1

A. Cost Parameters

The parameter values are shown in Table III, in which all cost parameters are the per unit values of χ, which is set to be 5.9×10^5 \$/MWh according to [31].

TABLE III
COST PARAMETERS FOR CAPACITY OPTIMIZATION

Cost parameters for capacity optimization		
χ	Construction cost	1.0
ψ	Maintenance cost	0.00001
α	Penalty cost for violation of the upper SOC limitation	0.002
β	Penalty cost for violation of the lower SOC limitation	0.004
δ	Cost for wind power curtailment	0.00021
ε	Cost for the shortage of discharge power	0.001
η	Penalty cost for overcharged power	0.001
φ	Penalty cost for over-discharged power	0.002

The cost parameters must be reasonable to improve the feasibility of this methodology. Hence, relevant theoretical basis is needed for parameter setting. Meanwhile, it should be pointed out that the idea of sizing methodology of BESS will not be influenced by the inevitable parameter deviations as long as the parameter deviations are within reasonable ranges.

Notably, frequent over-charge/-discharge may severely damage BESS to impact its lifetime. Thus, as a penalty cost, α and β are set to effectively limit over-charge/-discharge as follows.

$$\beta=\frac{\Delta\chi}{V_N\cdot\tau_d\cdot d_d} \tag{19}$$

where $\Delta\chi$ is the cost investment of 1 MWh battery, V_N is the amount of energy that can be cycled through a 1MWh battery during the lifetime. From Table III, it can be seen $\Delta\chi$ is equal to the value of χ. According to [32], due to various DOD, the total energy that can be cycled from the battery is approximately within [520, 710] MWh. τ_d is a comprehensive factor mainly including the round-trip efficiency and degradation of BESS. The degradation may impact chemical reaction in BESS to increase power loss, and τ_d is set as 0.85. Besides, with frequent over-discharge, the total energy usage during BESS lifetime may be significantly decreased to be 12.5% of the nominal value in the worst case scenario [32]. Whenever BESS discharges, the equivalently cost of per unit charge/discharge power is increasing. d_d demonstrates the averaged energy usage decrement considering frequent over-discharge, and its value is set as 56.25%. Accordingly, β can be calculated to be within [1738, 2373] \$/MWh. In this paper, 2360 \$/MWh (normalized value is 0.004) is selected. Subsequently, α can be set by referring to the value of β. In contrast with over-discharge, overcharge incurs less damage to BESS. In this paper, α is set to be 1180 \$/MWh (normalized value is 0.002).

The experiment data in [33] show that the useful capacity of BESS can be greatly decreased (20% of rated energy capacity at worst) when BESS discharges with a high rate, and the high rate charge can also incur potential damage to BESS. Subsequently, according to the analysis of parameters α and β, parameters φ can be computed in a similar manner.

$$\varphi=\frac{\Delta\chi}{V_N\cdot\tau_d}\cdot d_r \tag{20}$$

where d_r demonstrates the equivalent cost increment considering the impact of high discharge rate. Notably, cpf for power capacity determination guarantees that 95% of the discharge power is lower than the rated value. Furthermore, the set of maximal discharge power P^d_{max} in (4) can avoid sever damage from over-discharge. For this reason, d_r is determined as 1/95%. Accordingly, φ can be calculated to be within [929, 1238] \$/MWh. In this paper 1180 \$/MWh (normalized value is 0.002) is selected for φ. Subsequently, η can be set by referring to the value of φ. In this paper, η is set to be 590 \$/MWh (normalized value is 0.001).

Normally wind energy trading is implemented by power purchase agreement (PPA), which is a legal contract between an electricity generator (provider) and a power purchaser. Accordingly, the curtailed wind power can be evaluated by δ_r and $\Delta\delta$, in which δ_r is the PPA price and $\Delta\delta$ shows the cost of wear and tear.

$$\delta=\delta_r+\Delta\delta \tag{21}$$

According to the wind technologies market report in [34], δ_r is within the range [20,120] \$/MWh, so δ_r is selected to be 80 \$/MWh in this paper. In terms of $\Delta\delta$, its value is determined by the total installed wind power project cost divided by the total wind generation in the lifetime of wind farm.

$$\Delta\delta=\frac{c_{wf}\cdot s_{wf}}{365\cdot24\cdot N_{wf}\cdot e_w} \tag{22}$$

where c_{wf} is the installed wind power cost per unit size in \$/kWh. s_{wf} is the installed power of wind farm. N_{wf} is the lifetime of wind farm. e_w is the hourly average wind power generation in MWh. According to [34], c_{wf} is within [1600, 3000] \$/kWh due to various project size and regions, and N_{wf} is selected to be 20 years. Based on the annual wind power data, e_w of the selected 90 MW wind farm is about 31.7 MWh. Afterwards, $\Delta\delta$ is calculated to be within [25.9, 48.6] \$/MWh. In this paper, $\Delta\delta$ is selected to be 43.9 \$/MWh in this paper. Consequently, δ is finally determined to be 123.9 \$/MWh (normalized value is 0.00021).

In terms of ε, if the shortage of discharge power occurs, the wind farm not only needs to buy wind energy from electricity market to compensate the shortage of wind power, but also has to pay the penalty. Normally the penalty would be predetermined in the PPA contracts by electricity provider and purchaser. In this paper, considering the negative impact on frequency variation of wind power, the shortage of discharge power needs to be effectively constrained. Then ε is set as a relatively high value 590 \$/MWh (normalized value is 0.001).

B. Optimal Reference Output for Capacity Planning

The optimal reference output is verified by comparison between traditional hourly constant output and the proposed reference output. For comparison purpose, the wind power of typical days in summer and winter are chosen to show the simulation results. Figs.7 (a) shows the reference output for a typical day in summer, and Fig.7 (b) shows the reference output in winter.

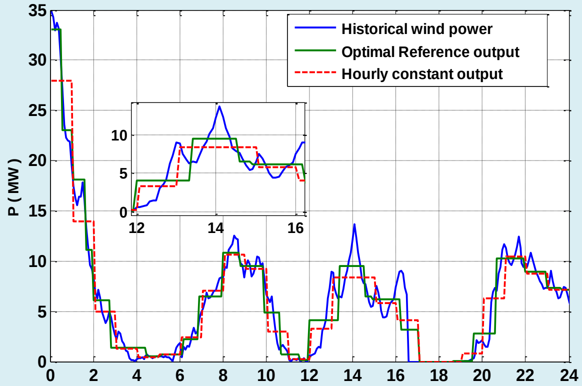

(a)

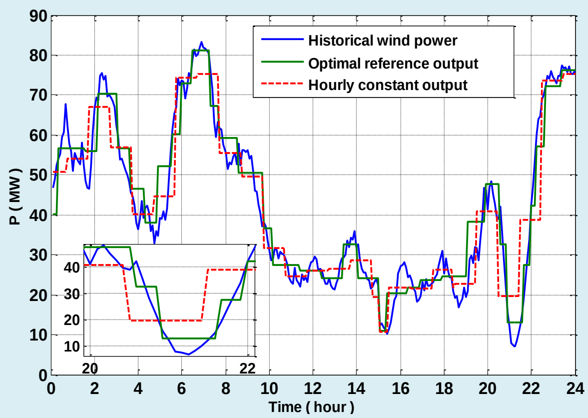

(b)

Fig. 7. Reference output of a typical day in (a) summer;(b)winter

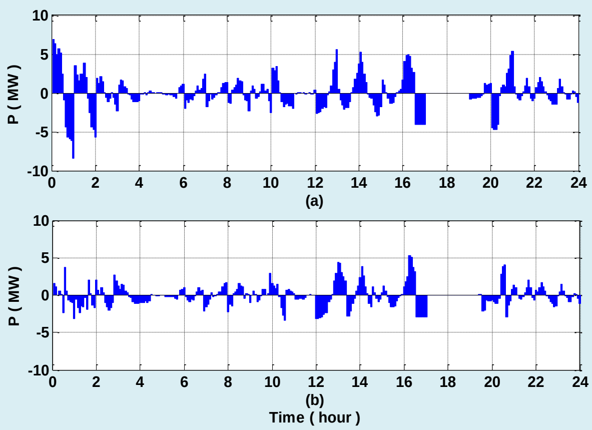

Fig. 8. Power deviation of a typical day in summer between wind power and (a) the hourly constant output; (b) the optimal reference output

Obviously, it can be seen that both in summer and winter the proposed optimal reference output can better track the wind power than the hourly constant output. In addition, the power deviation between the wind power and the reference outputs are shown in Fig. 8. Obviously the optimal reference output can produce smaller deviation than the hourly constant output, which also implies that less power needs to charge/discharge and lower power and energy capacity will be required. The same conclusion can be drawn from Fig. 9.

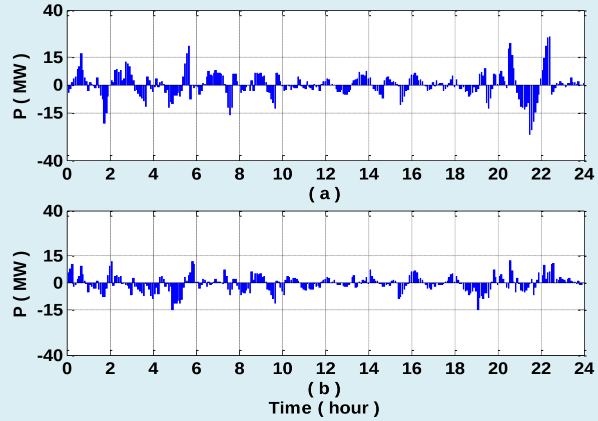

Fig. 9. Power deviation of a typical day in winter between wind power and (a) the hourly constant output; (b) the optimal reference output

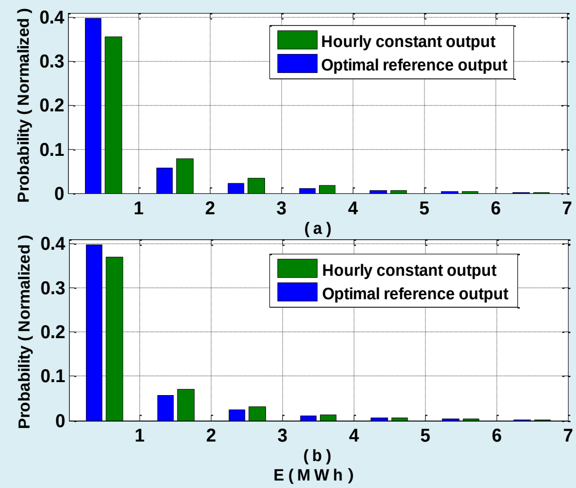

Fig. 10. Energy probability distribution. (a) Charge intervals; (b) discharge intervals.

For further verification, Fig. 10 (a) shows the probability distribution of charging energy of each charge interval. In low-energy charge intervals, which is lower than 1 MWh in this paper, the probability is nearly 40%, whereas the ratio is 35.8% for the hourly constant output. In high-energy sections, where the charge energies are more than 1 MWh, the probabilities of the optimal reference output are all lower than the hourly constant output. This means that the optimal reference output has more low-energy charge and less high-energy charge to reduce the total charge energy of BESS. Moreover, from Fig. 10 (b), it can also be seen that less discharge energy needs to be released in the optimal reference output. Since less charge and discharge energy of each interval are needed, less BESS energy capacity will be required in the presented sizing scheme.

Furthermore, single interval duration of the optimal reference output during the whole year is statistically calculated, and Fig. 11 shows its probability distribution. It is worth noting that more than 50% of the time intervals are within [0.75, 1] hour, and nearly 30% are within [1, 2] hours, but only less than 3% are smaller than 0.5 hour. In contrast with the hourly constant output, nearly 30% of the intervals are longer than 1 hour, which can greatly improve the reliability of the market trading and dispatchability level of wind power.

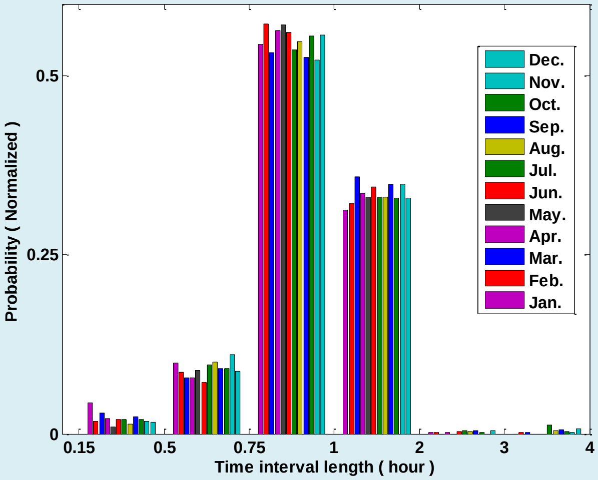

Fig. 11. Probability distribution of the time interval duration

C. BESS capacity determination

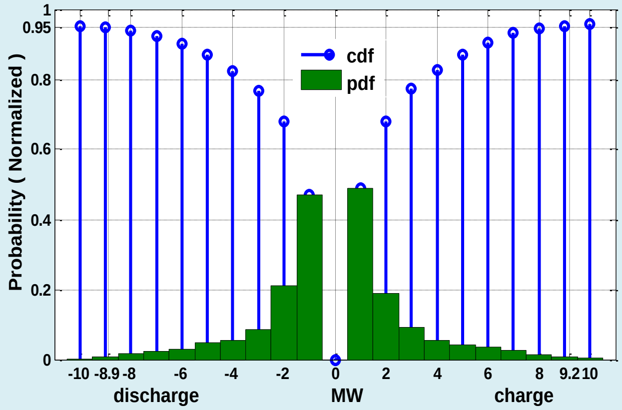

Fig. 12. pdf and cdf curves of the charge/discharge power

1) Power capacity: Fig. 12 shows the pdf and cdf curves of the charge/discharge power. When cpf is equal to p, the corresponding power can be defined as the rated charge/discharge power. Correspondingly, the rated charge power is 9.2 MW, while the rated discharge power is -8.9 MW.

2) Energy capacity: Table IV provides the comparison of energy capacities under different reference outputs and solver schemes.

TABLE IV
ENERGY CAPACITY COMPARISON

		Energy capacity (MWh)	
		Hourly constant output	Optimal reference output
Solver	PSO	28.5	23.4
	Improved PSO	26.6	22.1

In contrast with the hourly constant output, solved by the traditional PSO algorithm, the energy capacity with the optimal reference output is decreased to be 23.4 MWh. This verifies that the optimal referenced output can greatly reduce the energy capacity requirement. Meanwhile, with the improved PSO algorithm, the energy capacity is further decreased to be 22.1 MWh, which is defined as the rated energy capacity in this paper. Obviously, the improved PSO can also play a role in optimizing the rated energy capacity.

D. Smoothing performance

After smoothing the fluctuations of wind power, three indexes are defined in this paper as an evaluation scheme to verify the smoothing performance.

1) Deviation energy E_d. E_d is derived from the difference between the optimal reference output and the smoothed output, as shown in (23). E_d is used to evaluate the ability of BESS whether the wind power could be smoothed identically with the reference output.

$$E_d = \sum_{t=t_0}^{t_T} \left| P_t^{sw} - P_t^{ref} \right| \cdot \Delta t \tag{23}$$

2) Curtailed energy E_c. E_c is defined as the sum of the energy loss caused by wind power curtailment during the smoothing procedure.

$$E_c = \sum_{t=t_0}^{t_T} \left| P_t^{cw} \right| \cdot \Delta t \tag{24}$$

3) Frequency of SOC limit violation. G is introduced as the total times of the SOC limit violation in one whole year to evaluate the potential damage to BESS.

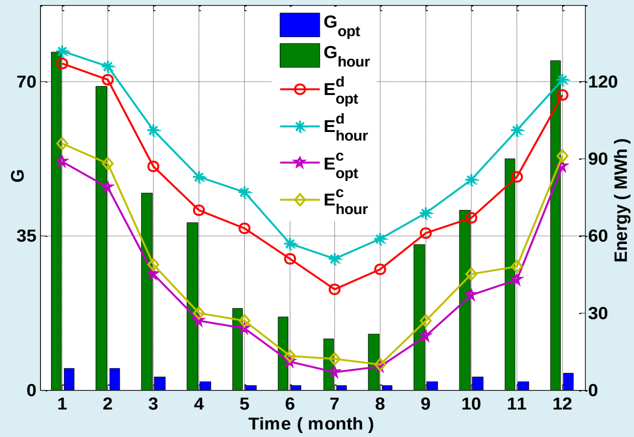

Fig. 13. Indicator parameter values of each month

Considering the seasonal features of wind power variations, monthly distributions of the indicator parameters are shown in Fig. 13, where E^d_{opt} , E^c_{opt} and G_{opt} are indicator parameters for the optimal reference output, and E^d_{hour}, E^c_{hour}, and G_{hour} are for hourly constant output. It can be seen that all curves appear similar trends. Specifically, the E^d_{opt} values are lower than E^c_{hour} , indicating that the power fluctuations are better mitigated with optimal reference output. E^c_{opt} has the same curve pattern as E^c_{hour}, but with smaller values, which implies that the wind power utilization can be promoted on basis of the proposed optimal reference output.

With respect to SOC, under the fuzzy control strategy of BESS, G_{opt} has been significantly decreased compared with G_{hour}. The first reason is that the fuzzy control strategy can adjust the charge/discharge power when SOC_t approaches warning lines. Another reason is that the charge/discharge powers have been constrained in (4) during the reference output optimization, so it can decrease the risk of limit violations of SOC as well. Thus, from indicator G, it can be observed that the SOH of BESS can be effectively protected by the proposed reference output and BESS control strategy.

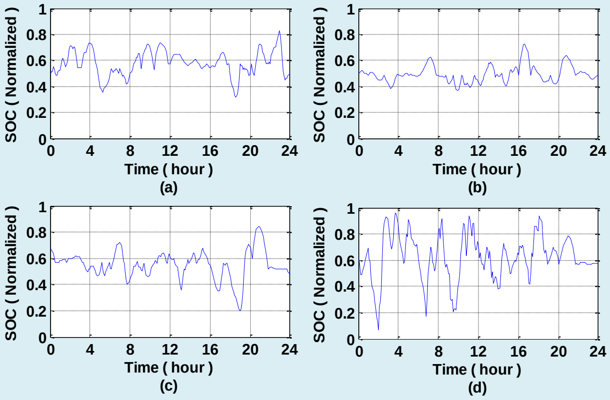

Fig. 14. SOC curves of typical days in each season. (a) Spring; (b) summer; (c) autumn; (d) winter.

The SOC curves of typical days in each season are chosen to show the evolution of SOC. From Fig.14, it can be seen that under various seasonal fluctuation patterns, BESS has been protected with the self-adaptive SOC control strategy, and SOC has been constrained within the reasonal ranges even in winter which has the severest fluctuations.

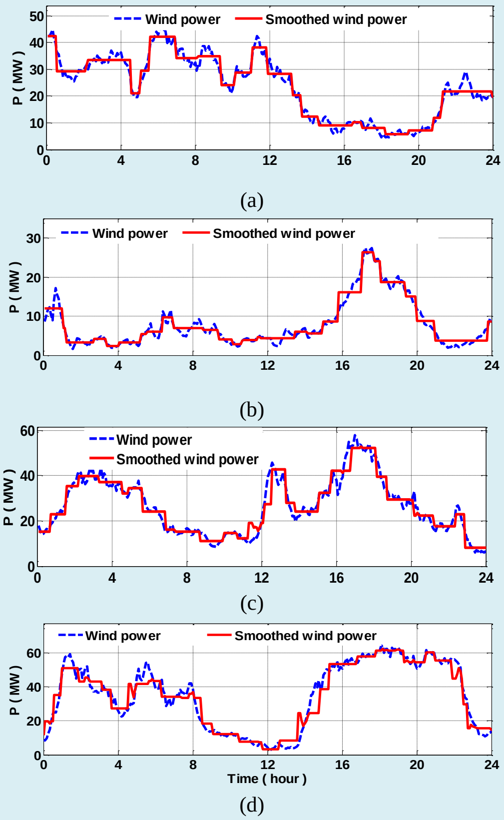

Fig. 15. Smoothed wind power of typical days in each season. (a) Spring; (b) summer; (c) autumn; (d) winter.

Furthermore, the smoothing performances of typical days in each season are shown in Fig. 15. Wind power fluctuations can be effectively mitigated even in winter. In addition, with the mild fluctuations in summer, the average time interval duration is much longer than the hourly output, and this will significantly benefit the market trading and dispatchability of the smoothed wind power.

To further verfy the planned BESS, wind power data of recent three years are collected to evaluate the performance of the BESS capacity. The index comparison are shown in Table V. Obviously, the BESS capacity determined with annual wind power can also have good performances in other year data, which also implies that based on annual period feature of wind power, the presented capacity planning methodology is convincing for application.

TABLE V
FURTHER VERIFICATION WITH OTHER THREE YEAR WIND POWER

Index	E_d (MWh)		E_c (MWh)		G	
	E^d_{opt}	E^d_{hour}	E^c_{opt}	E^c_{hour}	G_{opt}	G_{hour}
2013	926	1051	473	531	38	498
2014	910	1037	460	510	31	471
2015	915	1041	465	515	32	485

E. Cost-benefit analysis of BESS

From the point of view of wind farm owners, the purpose of installing BESS is to smooth wind power and benefit wind power trading. In contrast, if wind power is integrated into power grid without fluctuation smoothing, the wind farm will face penalty due to the power fluctuations. However, considering the high investment cost of BESS, it is still necessary to analyze the cost-benefit model of BESS to verify whether the increased profit obtained by BESS can justify the investment

As the generation schedule, reference output is reported to the TSO, and then wind power generation must track the reference power. With BESS, power gaps between wind power generation and the reference power can be smoothed to guarantee the generations schedule. In contrast, without BESS, wind farm has to take measures to track generation schedule. Specifically, when power generation is larger than the reference power, wind farm has to curtail the surplus wind power, and when power generation is smaller, wind farm has to face financial penalty due to the shortage of wind power. Subsequently, without BESS, the cost wind farm has to pay is shown as

$$C_{NOBESS} = \delta \cdot \sum_{i=1}^{nc} \sum_{t=nc_{0i}}^{nc_i} \left(P_t^w - P_i^{ref} \right) \cdot \Delta t + \varepsilon \cdot \sum_{j=1}^{nd} \sum_{t=nd_{0j}}^{nd_j} \left| P_t^w - P_i^{ref} \right| \cdot \Delta t \tag{25}$$

Accordingly, when BESS is intalled in wind farm, C_{NOBESS} can be avoided. Hence, if C_{NOBESS} is larger than the investment cost of BESS, it would verify that the profit obtained by BESS is worth the investment cost. According to the planned BESS energy capacity, $(\chi+\psi)\cdot V_{rat}$ can demonstrated the total investment cost. After calculation, the annual equivalent investment cost is 3.68 (normalized value). In contrast, using annual historical wind power data, C_{NOBESS} in (25) is calculated as 16.13 (normalized value). Apparently, the annual benefit obtained by BESS is much larger than the equivalent annual cost, which can validate that BESS is cost-effective for wind farm owners.

F. Real time operation of BESS

To verify the feasibility of BESS in real-time opreation, the smoothing performance of typical days including the forecasted wind power, actual wind power, reference power output and the smoothed wind power are shown in Fig.16. It should be noted that during the rolling operation of BESS, the reference output for the next time interval can be computed automatically in real time, and the self-adaptive control strategy still can protect BESS to avoid overcharge/over-discharge. Meanwhile, the smoothing performance can also be guaranteed to generate staircase power with flexible time durations. The wind power forecast data can be obtained by the forecast system in wind farm, which records the rolling forecast data of wind power. For comparison, diesel generator and vanadium redox battery (VRB) are chosen to address forecast power error separately. It verifies that both diesel generator and VRB can achieve the similar smoothing performances as Fig. 16.

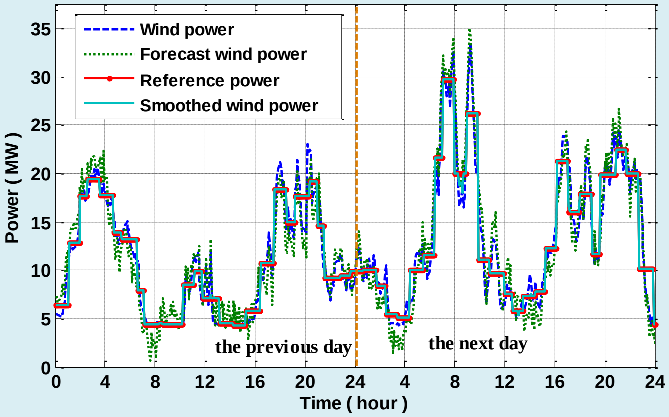

Fig.16 Real time operation of BESS

TABLE VI
COMPARISON BETWEEN DIESEL GENERATOR AND VRB

Index	Startup time	Capacity	Annual cost investment	Air pollution
Diesel generator	Seconds	2 MW	38000 $	Yes
VRB	Seconds	2 MW/ 1 MWh	45000 $	No

From Table VI, it can be seen that diesel generator is an excellent choice due to its quick startup and low cost. The cost is mainly composed by diesel generator, diesel consumption and curtailed wind power. VRB can also show a good performance in addressing forecast error. VRB has long life span, low maintenance requirements, and especially no constraints on charge/discharge switch [35], so it is quite suitable for the frequent variation of forecast power error.

From an economic point of view, the cost investment of diesel generator and VRB are both much smaller than BESS, so there is no concern on the increment of total investment cost.

VII. Conclusion

A novel BESS capacity planning methodology is proposed in this paper. By minimizing the power deviation between the wind power and reference output, an optimal reference output is presented to provide dispatchable wind power and reduce the BESS capacity requirement. Moreover, on basis of fuzzy control theory, a self-adaptive SOC control strategy is proposed to protect the SOH of BESS. Based on the optimal reference output and SOC control strategy, a statistical method for BESS power capacity calculation is presented; and then a cost-oriented model is formulated to determine the energy capacity of BESS. Case studies with historical wind power data are fulfilled to demonstrate that the determined BESS can effectively mitigate wind power fluctuations.

References

[1] C. Wan, Z. Xu, P. Pinson, Z. Y. Dong, and K. P. Wong, "Probabilistic forecasting of wind power generation using extreme learning machine," *IEEE Trans. Power Syst.*, vol. 29, no. 3, pp. 1033-1044, May. 2014.
[2] C. Wan, Z. Xu, and P. Pinson, "Direct interval forecasting of wind power," *IEEE Trans. Power Syst.*, vol. 28, no. 4, pp. 4877-4878, Nov. 2013.
[3] H. Bludszuweit and J. A. Domínguez-Navarro, “A probabilistic method for energy storage sizing based on wind power forecast uncertainty,” *IEEE Trans. Power Syst.*, vol. 26, no. 3, pp. 1651-1658, Aug. 2011.
[4] Y. Zheng, Z. Y. Dong, S. Huang, K. Meng, F. J. Luo, J. Huang, and D. HILL, “Optimal integration of mobile battery energy storage in distribution system with renewables,” *J. Mod. Power Syst. Clean Energy*, vol. 3, no. 4, pp. 589-596, Aug. 2015.
[5] P. Yang and A. Nehorai, “Joint optimization of hybrid energy storage and generation capacity with renewable energy,” *IEEE Trans. Smart Grid*, vol. 5, no. 4, pp. 1566-1574, Jul. 2014.
[6] A. S. A. Awad, J. D. Fuller, T. H. M. EL-Fouly, and M. M. A. Salama, “Impact of energy storage systems on electricity market equilibrium,” *IEEE Trans. Sustain. Energy*, vol. 5, no. 3, pp. 875- 885, Jul. 2014.
[7] A. Damiano, G. Gatto, I. Marongiu, M. Porru, and A. Serpi, “Real-time control strategy of energy storage systems for renewable energy sources exploitation,” *IEEE Trans. Sustain. Energy*, vol. 5, no. 2, pp. 567-576, Apr. 2014.
[8] J. C. Chen and X. D. Song, “ Economics of energy storage technology in active distribution networks,” *J. Mod. Power Syst. Clean Energy*, vol. 3, no. 4, pp. 583–588, Nov. 2015.
[9] L. Xu, X. B. Ruan, C. X. Mao, and B. H. Zhang, “An improved optimal sizing method for wind-solar-battery hybrid power system,” *IEEE Trans. Sustain. Energy.*, vol. 4, no. 3, pp. 774-785, Jul. 2013.
[10] F. Luo, K. Meng, Z. Y. Dong, Y. Zheng, Y. Chen and K. P. Wong, “Coordinated operational planning for wind farm with battery energy storage system,” *IEEE Trans. Sustain. Energy.*, vol. 6, no. 1, pp. 253-262, Jan. 2015.
[11] M. Ghofrani, A. Arabali, M. Etezadi-Amoli, and M. S. Fadali, “Energy storage application for performance enhancement of wind integration,” *IEEE Trans. Power Syst.*, vol. 28, no. 4, pp. 4803-4811, Nov. 2013.
[12] T. K. A. Brekken, A. Yokochi, A. e von Jouanne, and Z. Z. Yen, “Optimal energy storage sizing and control for wind power application,” *IEEE Trans. Sustain. Energy*, vol. 2, no. 1, pp. 69-77, Jan. 2011.
[13] D. L. Yao, S. S. Choi, K. J. Tseng, and T. T. Lie, “Determination of short-term power dispatch schedule for a wind farm incorporated with dual-battery energy storage scheme,” *IEEE Trans. Sustain. Energy*, vol.3, no. 1, pp. 74–84, Jan. 2012.
[14] X. Ke, N. Lu, and C. Jin, “Control and size energy storage systems for managing energy imbalance of variable generation resources,” *IEEE Trans. Sustain. Energy*, vol. 6, no. 1, pp. 70–78, Jan. 2015.
[15] W. C. Wu, J. H. Chen, B.M. Zhang and H. B. Sun, “A robust wind power optimization method for look-ahead power dispatch,” *IEEE Trans. Sustain. Energy*, vol. 5, no. 2, pp. 507-515, Apr. 2014.
[16] S. Teleke, M. E. Baran, S. Bhattacharya *et al.*, “Rule-based control of battery energy storage for dispatching intermittent renewable sources,” *IEEE Trans. Sustain. Energy*, vol. 1, no. 3, pp. 117-124, Oct. 2010.
[17] C. S. Hearn, M. C. Lewis, S. B. Pratap, R. E. Hebner, F. M. Uriarte, D. M. Chen, and R.G. Longoria, “Utilization of optimal control law to size grid-level flywheel energy storage,” *IEEE Trans. Sustain. Energy*, vol. 4, no. 3, pp. 611-618, Oct. 2013.
[18] J. D. Dogger, B. Roossien, and D. J. Frans, “Characterization of Li-Ion batteries for intelligent management of distributed grid-connected storage,” *IEEE Trans. Energy Convs.*, vol. 26, no. 1, pp. 256-263, Mar. 2011.
[19] Y. Zheng, Z. Y. Dong, F. J. Luo *et al*., “Optimal allocation of energy storage system for risk mitigation of DISCOs with high renewable penetrations,” *IEEE Trans. Power Syst.*, vol. 29, no. 1, pp. 212-220, Jan. 2014.
[20] Q. Y. Jiang, Y. Z. Gong and H. J. Wang, “A battery energy storage system dual-layer control strategy for mitigating wind farm fluctuations,” *IEEE Trans. Power Syst*., vol. 28, no. 3, pp. 3263-3273, Aug. 2013.

[21] S. Teleke, M. E. Baran, A. Q. Huang, S. Bhattacharya, and L. Anderson, "Control strategies for battery energy storage for wind farm dispatching," *IEEE Trans. Energy Convs.*, vol. 24, no. 3, pp. 725-732, Sep. 2009.

[22] K. Meng, H. M. Yang, Z. Y. Dong, W. X. Guo, F. S. Wen, and Z. Xu, "Flexible operational planning framework considering multiple wind energy forecasting service providers," *IEEE Trans. Sustain. Energy*, vol. 7, no. 2, pp. 708-717, Apr. 2016.

[23] Q. Wang, C. Y. Zhang, Y. Ding, G. Xydis, J. H. Wang, and Jacob Ǿtergaard, "Review of real-time electricity markets for integrating distributed energy resources and demand response," *Applied Energy*, vol. 138, pp. 695–706, Nov. 2014.

[24] K. W. Wee, S. S. Choi and D. M. Vilathgamuwa, "Design of a least-cost battery super-capacitor energy storage system for realizing dispatch-able wind power," *IEEE Trans. Sustain. Energy*, vol. 4, no. 3, pp. 786-795, Jul. 2013.

[25] H. T. Le, S. Santoso, and T. Q. Nguyen, "Augmenting wind power penetration and grid voltage stability limits using ESS: application design, sizing, and a case study," *IEEE Trans. Power Syst*., vol. 27, no. 1, pp. 161- 171, Feb. 2012.

[26] M. A. Montes de Oca, T. Stützle, M. Birattari, and M. Dorigo, "Frankenstein's PSO: a composite particle swarm optimization algorithm," *IEEE Trans. Evol. Comput.*, vol. 13, no. 5, pp. 1120-1132, Oct. 2009.

[27] J. Ebrahimi, S. H. Hosseinian, and G. B. Gharehpetian, "Unit commitment problem solution using shuffled frog leaping algorithm," *IEEE Trans. Power Syst.*, vol. 26, no. 2, pp. 573-581, May. 2011.

[28] Q. Li, S. S. Choi, Y. Yuan, and D. L. Yao, "On the determination of battery energy storage capacity and short-term power dispatch of a wind farm," *IEEE Trans. Sustain. Energy*, vol. 2, no. 2, pp. 148–158, Jan. 2011.

[29] S. Teleke, M. E. Baran, S. Bhattacharya *et al.*, "Rule-based control of battery energy storage for dispatching intermittent renewable sources," *IEEE Trans. Sustain. Energy*, vol. 1, no. 3, pp. 117-124, Oct. 2010.

[30] M. Y. Suberu, M. W. Mustafa, and N. Bashir, "Energy storage systems for renewable energy power sector integration and mitigation of intermittency," *Renewable and Sustainable Energy Reviews.*, vol. 35, pp. 499–514, Jul. 2014.

[31] K. C. Divya and J. Ǿtergaard, "Battery energy storage technology for power systems—an overview," *Electric Power Systems Research*, vol. 79, pp. 511–520, May. 2009.

[32] H. W. Bindner, T. Cronin, P. Lundsager, J. F. Manwell, U. Abdulwahid, and I. Baring-Gould, "Lifetime modelling of lead acid batteries," Risø National Laboratory, Technical University of Denmark, Roskilde Denmark, Apr. 2005.

[33] Igor Papič, "Simulation model for discharging a lead-acid battery energy storage system for load leveling," *IEEE Trans. Energy Convs.*, vol. 21, no. 2, pp. 608-615, Jun. 2006.

[34] R. Wiser, L. Berkeley, and M. Bolinger, "2014 Wind technologies market report," U. S. Department of Energy, Springfield, Illinois, TN 37831-0062, Aug. 2015.

[35] T. A. Nguyen, M. L. Crow, and A. C. Elmore, "Optimal sizing of a vanadium redox battery system for microgrid systems," *IEEE Trans. Sustain. Energy*, vol. 6, no. 3, pp. 74–84, Jul. 2015.

Feng Zhang (M'11) received his Ph.D. degree from Shandong University, China, in 2011.

He is currently with School of Electrical Engineering, Shandong University, Jinan, China. He was a visiting Ph.D. student in the University of Manchester, UK. During 2015 and 2016, he was a Research Associate at Department of Electrical Engineering, The Hong Kong Polytechnic University. His research interests include renewable energy, micro-grid, energy storage, and economic dispatch of power system.

Ke Meng (M'10) obtained Ph.D. from the University of Queensland, Australia in 2009. He is currently with the School of Electrical and Information Engineering, The University of Sydney, Australia. Before that, he was a research academic with the center for intelligent electricity networks, the University of Newcastle, Australia. He is also a visiting Professor of the Changsha University of Science and Technology. His research interest includes pattern recognition, power system stability analysis, wind power, and energy storage.

Zhao Xu (M'06-SM'13) received his B.Eng., M.Eng, and Ph.D. degrees from Zhejiang University, China, in 1996, National University of Singapore, Singapore, in 2002, and The University of Queensland, Australia, in 2006, respectively.

He is now with The Hong Kong Polytechnic University. He was previously with Centre for Electric Power and Energy, Technical University of Denmark. His research interest includes demand side, grid integration of renewable energies and EVs, electricity market planning and management, and AI applications in power engineering. He is an Editor of IEEE Transactions on Smart Grid, IEEE POWER ENGINEERING LETTERS, and Electric Power Components and Systems journal.

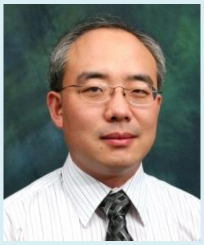

Zhao Yang Dong (M'99-SM'06) obtained his Ph.D. degree from the University of Sydney, Australia in 1999. He is now Professor and Head of School of Electrical and Information Engineering, University of Sydney, Australia. He was previously Ausgrid Chair and Director of the Center for Intelligent Electricity Networks (CIEN), The University of Newcastle, Australia, and is now a conjoint professor there. He also held academic and industrial positions with the Hong Kong Polytechnic University and Transend Networks (now TASNetworks), Tasmania, Australia. His research interest includes Smart Grid, power system planning, power system security, load modeling, electricity market, and computational intelligence and its application in power engineering. Prof. Dong is an editor of IEEE Transactions on Smart Grid, IEEE Transactions on Sustainable Energy, IEEE Power Engineering Letters, and IET Renewable Power Generation.

Li Zhang obtained her BSc. from Tianjin University in 1989, her MSc. and Ph.D from Shandong University of Technology in 1992 and Shandong University in 2006, respectively. Currently she is an associate professor at Shandong University, Jinan, China. Her research interests include economic operation of power system and electricity market.

Can Wan (M'15) received his B.Eng. and Ph.D. degrees from Zhejiang University, China, in 2008, and The Hong Kong Polytechnic University in 2015, respectively. He is with College of Electrical Engineering, Zhejiang University, Hangzhou, China. He was a Postdoc Fellow at Department of Electrical Engineering, Tsinghua University, Beijing, China, and a Research Associate at Department of Electrical Engineering, The Kong Hong Polytechnic University. He was a visiting scholar at the Center for Electric Power and Energy, Technical University of Denmark, and Argonne National Laboratory, IL, USA. His research interests include forecasting, power system analysis and operation, renewable energy, active distribution network, demand side, and machine learning.

Jun Liang received his Ph.D. degree from the School of Electrical Engineering at Shandong University, Jinan, China. He is currently a Professor at Shandong University. His research interest is power system analysis and operation.